

Cite this: *Dalton Trans.*, 2021, **50**, 3931

Copper(II) complexes of *N*-propargyl cyclam ligands reveal a range of coordination modes and colours, and unexpected reactivity†

Andrew J. Counsell, ^a Mingfeng Yu, ^b Mengying Shi,^a Angus T. Jones,^a James M. Batten, ^a Peter Turner,^a Matthew H. Todd ^{*c} and Peter J. Rutledge ^{*a}

The coordination chemistry of *N*-functionalised cyclam ligands has a rich history, yet cyclam derivatives with pendant alkynes are largely unexplored. This is despite the significant potential and burgeoning application of *N*-propargyl cyclams and related compounds in the creation of diversely functionalised cyclam derivatives via copper-catalysed azide–alkyne ‘click’ reactions. Herein we describe single crystal X-ray diffraction and spectroscopic investigations of the coordination chemistry of copper(II) complexes of cyclam derivatives with between 1 and 4 pendant alkynes. The crystal structures of these copper complexes unexpectedly reveal a range of coordination modes, and the surprising occurrence of five unique complexes within a single recrystallisation of the tetra-*N*-propargyl cyclam ligand. One of these species exhibits weak intramolecular copper–alkyne coordination, and another is formed by a surprising intramolecular copper-mediated hydroalkoxylation reaction with the solvent methanol, transforming one of the pendant alkynes to an enol ether. Multiple functionalisation of the tetra-*N*-propargyl ligand is demonstrated via a ‘tetra-click’ reaction with benzyl azide, and the copper-binding behaviour of the resulting tetra-triazole ligand is characterised spectroscopically.

Received 30th October 2020,
Accepted 21st January 2021

DOI: 10.1039/d0dt03736b

rsc.li/dalton

Introduction

Cyclam **1** (Fig. 1) and *N*-functionalised cyclam derivatives have a long and distinguished history as macrocyclic ligands that give rise to metal complexes with diverse and interesting properties, with their coordination modes, reactivity, and bioactivity continuing to draw sustained research interest.^{1–4}

Functionalisation of one or more of the secondary amines in the azamacrocycle is easily achieved, affording diverse and significant changes to the properties of the resulting ligand and metal complexes. The variance of their properties depends primarily upon the degree of amine substitution, the electronic and steric properties of the *N*-substituents, the metal cation, the nature of anionic species present during complexation, and pH.³ The resultant versatility has enabled the application of cyclam derivatives across a wide range of areas including

chemosensing,^{5,6} biomimicry,^{7,8} molecular switches,^{9,10} supramolecular systems,^{11,12} catalysis,^{13–15} and medicine.^{16–19}

Pendant groups including amine, alcohol, thiol, ester, carboxylic acid, amide, carbamate, urea, sulfonamide, nitrile, thioester, pyridyl, triazolyl and phosphonate functionality have been incorporated in side-arms of varying length and complexity,^{2,3} to modulate properties such as chelate effects, the selectivity of metal ion-binding, side-chain reactivity, and pendant lability. From the simple aminoethyl derivative **2** used to study the pH-dependence of side-chain coordination to a chelated nickel ion,²⁰ this field has expanded to include compounds such as the dansylate **3** cast as the basis for a light-emitting molecular machine,¹⁰ the likes of naphthalimide derivative **4** which incorporate fluorescent dyes for metal ion sensing,^{21–23} and molecules of general structure **5**, which have demonstrated potency against drug-resistant *Mycobacterium tuberculosis* (Fig. 1).^{24,25} Relatively little attention has been paid to cyclam derivatives bearing alkyne pendant groups and the metal complexes they form. The recently reported surface modification of glassy carbon electrodes for CO₂ reduction with a series of [Ni(alkynyl-cyclam)]²⁺ complexes serves as an isolated example.²⁶

We have ongoing interests in *N*-propargyl cyclams as precursors for Cu(I)-catalysed azide–alkyne Huisgen ‘click’ reactions, which enable the introduction of more complex pendant func-

^aSchool of Chemistry, The University of Sydney, Sydney, New South Wales 2006, Australia. E-mail: peter.rutledge@sydney.edu.au; Tel: +61 2 9351 5020

^bDrug Discovery and Development, Cancer Research Institute, Clinical and Health Sciences, University of South Australia, Adelaide, South Australia 5001, Australia

^cSchool of Pharmacy, University College London, 29-39 Brunswick Square, London WC1N 1AX, UK. E-mail: matthew.todd@ucl.ac.uk; Tel: +44 207 753 5568

† Electronic supplementary information (ESI) available. CCDC 2012628–2012634 and 2019803. For ESI and crystallographic data in CIF or other electronic format see DOI: 10.1039/d0dt03736b

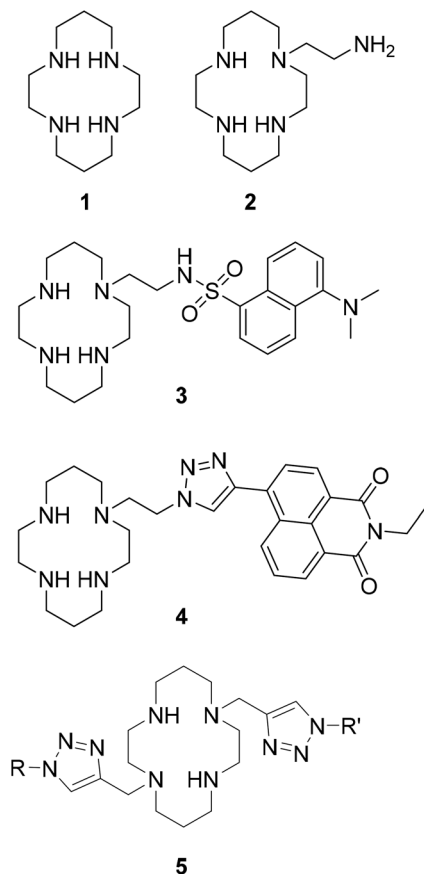


Fig. 1 Cyclam **1** and derivatives **2–5** with pendant ligands that have a broad range of applications.

tionality as in **4** and **5** above,^{27–29} a strategy that has also been employed in a number of other metal chelating systems.³⁰

Herein we report the structural characterisation of the copper complexes of *N*-propargyl cyclams **6–9** bearing 1–4 pendant alkynes (Fig. 2). This group of ligands was chosen to probe the effect that the degree of amine substitution, and the electronic and steric properties of the *N*-substituents, have upon the structures of the Cu(II) complexes. The complexes exhibit an interesting variety of alkyne coordination modes and stereochemistry across the series and individually. Structures of the Cu(II) complexes of **6–9** are reported, including a series of the Cu(II) complex obtained from a single recrystallisation, and an unexpected enol ether complex derived from the reaction of Cu(II) with methanol solvent.

Results and discussion

Synthesis of ligands and metal complexes

Preparation of the mono *N*-propargyl cyclam **6** proceeded in good overall yield (68%) from cyclam **1** (Scheme 1 and Scheme S1, ESI†) using previously reported methods.^{26,31,32} The bis-alkyne derivative **7** was obtained through conversion of cyclam **1** to a bis-aminal-bridged intermediate (Scheme S1,

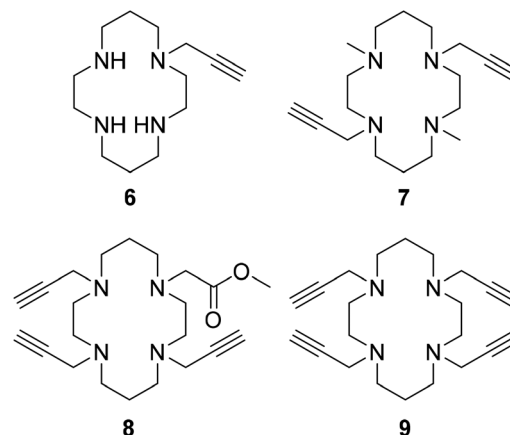


Fig. 2 Functionalised cyclam ligands **6–9** bearing pendant alkynes.

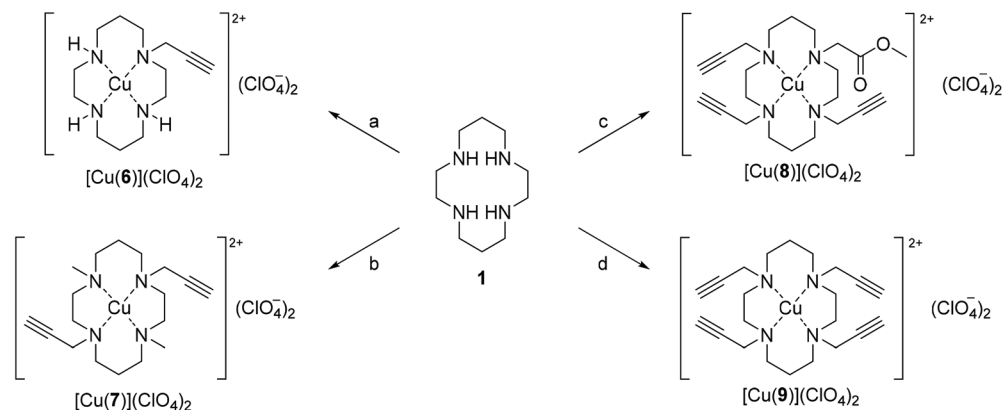
ESI†), which was alkylated, deprotected with basic work-up,^{29,33} and then methylated with an Eschweiler–Clarke reaction to form **7** in good overall yield (62%).

Initial attempts to synthesise **8** *via* alkylation of tri-Boc cyclam with methyl bromoacetate failed at the deprotection stage. Once the tri-Boc/ester intermediate **10** is unmasked and exposed to the basic conditions used in the reaction with propargyl bromide, mono *N*-alkylated cyclam **11** is prone to an intramolecular cyclisation reaction forming bicyclic lactam **12** (Scheme 2), as reported previously for the ethyl ester analogue of **11** and related systems.^{34,35} Ligand **8** was instead obtained directly from cyclam **1** *via* a one-pot synthesis with the slow, sequential addition of propargyl bromide and methyl bromoacetate in strict 3:1 stoichiometry under basic conditions (Scheme 1) in a poor but tolerable yield (10%). The tetrapropargyl ligand **9** was prepared in good yield (72%) using the direct, one-step tetra-*N*-alkylation reaction we have recently reported, with propargyl bromide and a base in a ‘miscible biphasic’ system.³⁶

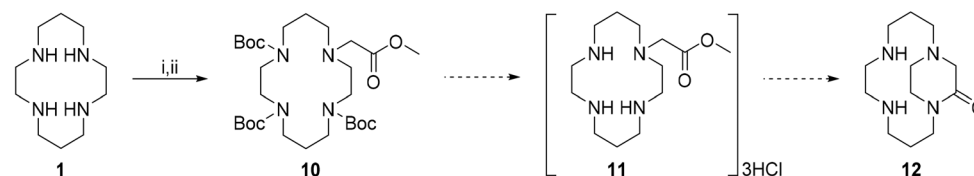
Metal complexes were prepared by dissolving each of the ligands **6–9** in ethanol with copper(II) perchlorate and heating at reflux for one hour, then cooling on ice to precipitate the complex. This procedure, adapted from one we have previously reported for related systems,^{24,37} afforded the metal complexes [Cu(**6**)](ClO₄)₂·CH₃OH, [Cu(**7**)](ClO₄)₂·H₂O, [Cu(**8**)](ClO₄)₂·H₂O, and [Cu(**9**)](ClO₄)₂ in high yields (77–81%).

Structural characterisation of mono-, di- and tri-propargyl complexes

Single crystals of the Cu(II) perchlorate complexes of ligands **6**, **8** and **9** were obtained either through the slow diffusion of an aqueous Cu(ClO₄)₂ phase with a methanolic phase containing the ligand, or *via* the slow evaporation of a methanolic solution of the complex. Attempts to crystallise [Cu(**7**)](ClO₄)₂ from methanol were unsuccessful, and this was instead accomplished *via* the slow evaporation of a solution of the complex in acetonitrile. Structure determination and crystallographic details are provided electronically as part of the ESI.†



Scheme 1 Synthesis of ligands 6–9 and their copper complexes. Reagents and conditions: a. (i) (Boc)₂O, Et₃N, CH₂Cl₂, –15 °C to rt, 16 h, 77%; (ii) BrCH₂C≡CH, Na₂CO₃, rt, 16 h, 95%; (iii) TFA/CH₂Cl₂ (1 : 5), rt, 72 h, 93%; (iv) Cu(ClO₄)₂·6H₂O, EtOH, reflux, 1 h, 80%; b. (i) CH₂O, H₂O, rt, 16 h, 76%; (ii) BrCH₂C≡CH, CH₃CN, rt, 16 h, 90%; (iii) CH₂O, HCO₂H, H₂O, reflux, 24 h, 90%; (iv) Cu(ClO₄)₂·6H₂O, EtOH, reflux, 1 h, 81%; c. (i) BrCH₂C≡CH (3.0 eq.), BrCH₂CO₂CH₃ (1.0 eq.), Na₂CO₃, CH₃CN, reflux, 16 h, 10%; (ii) Cu(ClO₄)₂·6H₂O, EtOH, reflux, 1 h, 77%; d. (i) BrCH₂C≡CH, H₂O/CH₃CN (1 : 1), NaOH, rt, 16 h, 72%; (ii) Cu(ClO₄)₂·6H₂O, EtOH, reflux, 1 h, 80%. See Scheme S1 and synthesis and characterisation section of the ESI† for further details.



Scheme 2 Attempted synthesis of 8 via 10 was unsuccessful as the mono-*N*-alkyl cyclam 11 cyclises to the bicyclic lactam 12 in alkaline solution. Reagents and conditions: (i) (Boc)₂O, Et₃N, CH₂Cl₂, –15 °C to rt, 16 h, 77%; (ii) BrCH₂CO₂CH₃, Na₂CO₃, rt, 16 h, 95%; then deprotection with 2 M HCl in 1,4-dioxane, rt, and attempted alkylation with BrCH₂C≡CH and Na₂CO₃, rt. Cyclised product 12 was not isolated, but has been reported previously to form under similar conditions, see text for further details.

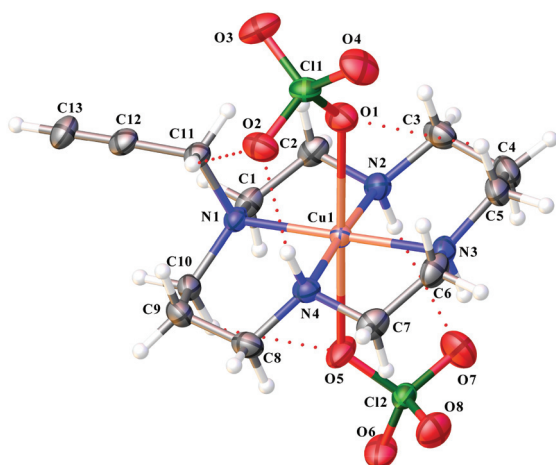


Fig. 3 Olex2 depiction of *trans*-III-[Cu(6)](ClO₄)₂, with displacement ellipsoids shown at the 50% level. A disordered methanol solvate molecule is not shown.

Complex [Cu(6)](ClO₄)₂ adopts a slightly distorted octahedral geometry, with weak axial perchlorate coordination to the metal centre (Fig. 3 and ESI Fig. SX1,† Table 1 and Table SX1†). The Cu–N macrocyclic amine distances vary from

Table 1 Selected bond distances (Å) within the metal coordination sphere observed in structures of the *N*-propargyl cyclam complexes [Cu(6)](ClO₄)₂, [Cu(7)](ClO₄)₂, and [Cu(8)](ClO₄)₂

	[Cu(6)](ClO ₄) ₂	[Cu(7)](ClO ₄) ₂	[Cu(8)](ClO ₄) ₂
Cu–O1 ^a	2.5170(18)		
Cu–O5 ^a	2.5403(18)		
Cu–N1	2.0802(19)	2.126(3)	2.1071(19)
Cu–N2	2.015(2)	2.074(3)	2.0615(18)
Cu–N3	2.0281(19)	2.111(3)	2.0844(18)
Cu–N4	2.008(2)	2.081(3)	2.0529(17)
Cu–N1S ^b		2.229(3)	
Cu–O1 ^c			2.2477(15)

^a O of perchlorate. ^b N of solvent (acetonitrile). ^c Carbonyl O of pendant ester.

2.008(2) to 2.0802(19) Å, similar to the theoretical expectation of 2.07 Å.³⁸ The relatively long metal to oxygen axial bond lengths of 2.5170(18) and 2.5403(18) Å reflect the character of perchlorate ion, and presumably Jahn–Teller distortion. The angles formed between the macrocycle nitrogen, metal, and perchlorato oxygen sites range from 85.37(7) to 94.37(7)° for one perchlorate counterion and 84.77(8) to 95.08(7)° for the second. The perchlorato oxygen to metal to *trans* perchlorato

oxygen angle is $177.50(6)^\circ$. The metal ion is displaced $0.023(1)$ Å from the least squares plane defined by the equatorial nitrogen atoms, $0.010(1)$ Å from the line defined by one of the pairs of opposing nitrogens (N1, N3), and $0.058(1)$ Å from that of the second pair (N2, N4).

Following chelation of a metal ion, a cyclam complex will adopt one of five configurations according to the spatial orientations of the backbone amine substituents: *RSRS*, *RRRS*, *SSRR*, *RSSR* and *RRRR*, respectively termed *trans-I* to *trans-V* (where the arrangement of cyclam nitrogens is planar); or a corresponding *cis* form (where the cyclam is 'folded')—noting that some forms will be highly strained and/or impossible to adopt.³⁹ The cyclam fragment $[\text{Cu}(6)]^{2+}$ adopts the preferred *trans-III* configuration, with adjacent *N*-alkyl substituents (R-N(CH₂)₃-N-R) displaced from the Cu-N plane. In spite of the tendency for similar complexes to exhibit metal-alkyne coordination,^{40–42} no such interaction is observed here between the *N*-propargyl group (C11–C13) and the metal centre.

As is the case with $[\text{Cu}(6)]^{2+}$, the single crystal structure of the $[\text{Cu}(7)(\text{CH}_3\text{CN})]^{2+}$ complex dication lacks coordination of the propargyl substituent to the metal centre (Fig. 4 and ESI Fig. SX2†). The presence of acetonitrile, a softer and more effective Lewis base, evidently precludes axial perchlorate coordination; the macrocyclic complex is essentially five coordinate with an apical copper(II) to acetonitrile nitrogen bond length of $2.229(3)$ Å (see also Table 1). There appears to be a weak—presumably electrostatic—interaction between the metal ion and the oxygen of a perchlorate anion *trans* to the acetonitrile, with the metal ion to oxygen site distance being $3.914(4)$ Å. The metal coordination environment is distorted square-pyramidal, with a trigonal index (τ) of 0.34 (where τ ranges from 0 to 1, indicating the extent of transition from the ideal square pyramidal to ideal trigonal bipyramidal geometries, respectively).⁴³ The metal is displaced $0.276(1)$ Å from the least squares plane defined by the equatorial nitrogen atoms, 0.095

(1) Å from the line defined by one of the pairs of opposing nitrogen atoms (N1, N3), with both in this pair bearing an alkyne residue, and $0.458(1)$ Å from that of the second pair (N2, N4). The $[\text{Cu}(7)(\text{CH}_3\text{CN})]^{2+}$ complex dication adopts the *trans-I* configuration.⁴⁴

Like the $[\text{Cu}(7)(\text{CH}_3\text{CN})]^{2+}$ complex dication, the single crystal structure of $[\text{Cu}(8)]^{2+}$ is essentially five coordinate (Fig. 5 and ESI Fig. SX3†), with a distorted square pyramidal coordination sphere and a *trans-I* configuration.⁴⁴ Here though, axial ligation involves the carbonyl oxygen of the pendant methyl ester, with a bond length of $2.2477(15)$ Å (Table 1). There is a significant distortion of the coordination geometry, with the macrocycle nitrogen to metal to axial oxygen angles ranging from $78.14(7)$ to 102.41° . This distortion is further reflected in the τ value of 0.35. The metal to macrocycle nitrogen distances vary from $2.0529(17)$ to $2.1071(19)$ Å. There again appears to be a weak interaction, presumably primarily electrostatic, between the metal cation and a perchlorate counterion *trans* to the pendant carbonyl oxygen, separated by $3.649(2)$ Å. The metal is displaced $0.222(1)$ Å from the least squares plane defined by the equatorial nitrogen atoms, $-0.078(1)$ Å from the line defined by one of the pairs of opposing nitrogen atoms (N1, N3), and $0.447(1)$ Å from that of the second pair (N2, N4). The negative offset indicates displacement towards the nitrogen equatorial plane.

Tetra-propargyl ligand 9 forms several different Cu(II) complexes

The crystallisation of $[\text{Cu}(9)](\text{ClO}_4)_2$ produced five visibly distinct crystals in the crystal growth flask (Fig. 6). The crystals were obtained *via* slow liquid–liquid diffusion overnight at

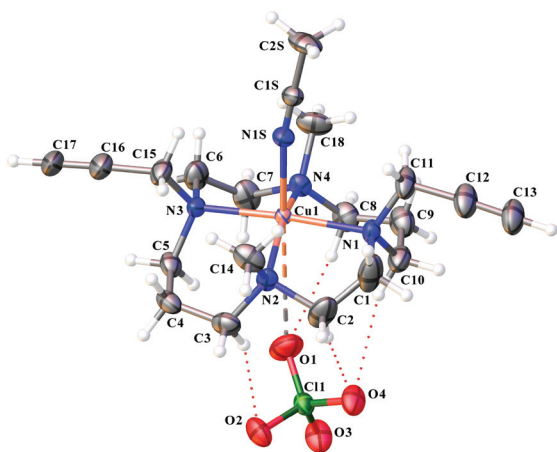


Fig. 4 Olex2 depiction of *trans-I*- $[\text{Cu}(7)(\text{CH}_3\text{CN})](\text{ClO}_4)^+$, with ellipsoids shown at the 50% probability level. The second perchlorate counterion is not shown.

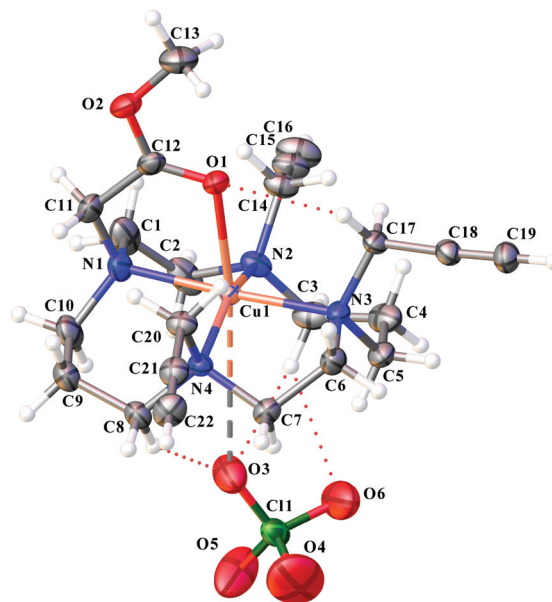


Fig. 5 Olex2 depiction of *trans-I*- $[\text{Cu}(8)](\text{ClO}_4)^+$, with ellipsoids shown at the 50% probability level. The second perchlorate counterion is not shown.

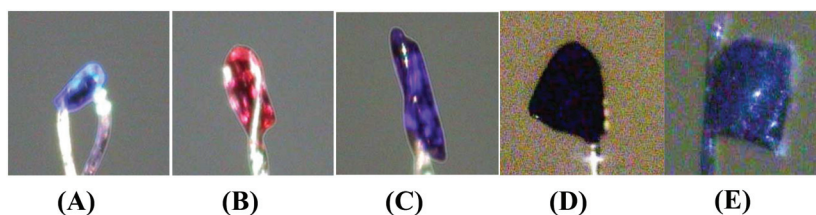


Fig. 6 Photographs of crystals isolated following the slow diffusion of aqueous $\text{Cu}(\text{ClO}_4)_2$ with a methanolic solution of **9**: (**9A**) *trans*-I-[Cu(**9**)](ClO_4)₂; (**9B**) *trans*-III-[Cu(**9**)](ClO_4)₂; (**9C**) *trans*-I/III-[Cu(**9**)](ClO_4)₂·H₂O; (**9D**) *trans*-I-[Cu(1,4,8-propargyl-11-(2-methoxypropene)cyclam)](ClO_4)₂·H₂O and (**9E**) *trans*-I-[Cu(1,4,8-propargyl-11-(2-methoxypropene)cyclam)](ClO_4)₂·0.25CH₃OH.

room temperature, of a 0.1 M aqueous solution of $\text{Cu}(\text{ClO}_4)_2$, with a 0.1 M methanolic solution of **9**. Distinguished here with labels **9A** to **9E**, the structures obtained from each exhibit significant variation in donor ligand configuration, conformation and even the ligand species, which was surprising given each complex assembly occurred from a single set of components under identical conditions.

Crystal **9A** was found to comprise a *trans*-I-[Cu(**9**)](ClO_4)⁺ complex cation (Fig. 7 and ESI Fig. SX4, Table 2 and Table SX2†). The structure geometry is five-coordinate square pyramidal ($\tau = 0.03$), with an axial perchlorate ligand and a coordinated cyclam adopting the favourable *trans*-I configuration. The metal is displaced 0.206(1) Å from the least squares plane defined by the equatorial nitrogen atoms, 0.219(1) Å from the line defined by one of the pairs of opposing nitrogen atoms (N1, N3), and 0.192(1) Å from that of the second pair (N2, N4).

The metal ion to cyclam nitrogen distances vary from 2.0711(17) to 2.1274(17) Å (Table 2). The coordinated perchlorate anion is disordered over two orientations (Fig. SX4, ESI†), with coordination bond lengths of 2.359(9) Å for the major component and 2.301(17) Å for the minor component. The complex cation is pseudo-oligomeric, with the copper of one

Table 2 Selected bond lengths (Å) and angles (°) within the metal coordination sphere observed in structures of the complex [Cu(**9**)](ClO_4)₂, **9A–9C**

	9A <i>trans</i> -I	9B ^a <i>trans</i> -III	9C	
			<i>trans</i> -I 9C-1	<i>trans</i> -III 9C-2 ^e
Cu–N1	2.0711(17)	2.1127(16)	2.059(2)	2.028(2)
Cu–N2	2.0959(18)	2.0283(15)	2.061(2)	2.125(2)
Cu–N3	2.0999(18)		2.063(2)	
Cu–N4	2.1274(17)		2.069(2)	
Cu–O ^b	2.359(9) ^d		2.890(2)	
Cu–O ^b	2.301(17) ^d			
Cu–alkyne ^c		2.93	3.04	2.93
N1–Cu–N2	93.87(7)	93.40(6)	94.09(9)	93.87(9)
N1–Cu–N3	167.92(7)		169.76(8)	
N1–Cu–N4	85.06(7)		86.57(9)	
N2–Cu–N3	84.87(7)		86.41(9)	
N2–Cu–N4	169.55(7)		163.81(8)	
N3–Cu–N4	94.00(7)		95.81(9)	
N1–Cu1–O ^b			98.48(7)	
N2–Cu1–O ^b			81.49(7)	
N3–Cu1–O ^b			91.72(7)	
N4–Cu1–O ^b			82.41(7)	

^a Third and fourth nitrogen sites generated through inversion operation $1 - x, 1 - y, 1 - z$. ^b Oxygen sites of perchlorate. ^c Metal to alkyne centroid distance. ^d Disordered perchlorate. ^e Third and fourth nitrogen sites generated through inversion operation $-x, 1 - y, -z$.

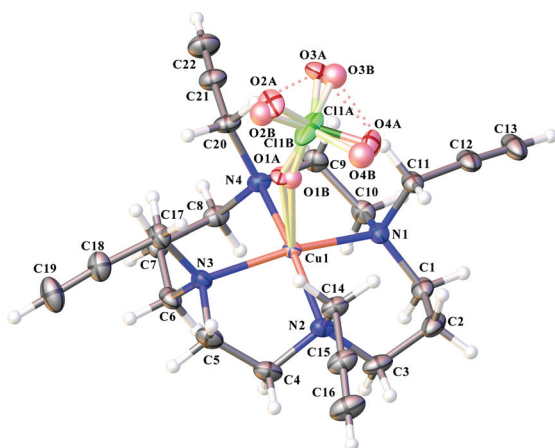


Fig. 7 Olex2 depiction of complex cation **9A**, *trans*-I-[Cu(**9**)](ClO_4)⁺, with displacement ellipsoids shown at 50% probability level. Disordered sites are highlighted with 'faded' colours. The second perchlorate counterion is not shown.

complex cation weakly interacting with the coordinated perchlorate of a second (Fig. SX5, ESI†), with metal to neighbouring perchlorate oxygen distances of approximately 3.51 Å for the major perchlorate orientation and 3.68 Å for the minor orientation.

Crystal **9B** was found to comprise a pseudo-octahedral *trans*-III-[Cu(**9**)]²⁺ complex dication in which axial ligation involves weak alkyne π system coordination. Located on an inversion centre, the complex dication has symmetrical bond lengths of approximately 2.93 Å (Fig. 8, Table 2 and ESI Fig. SX6, Table SX2†). Observation of the *trans*-III isomer of *tetra*-*N*-substituted cyclam derivatives is relatively unusual, with adoption of this spatial arrangement highly dependent on solvent conditions and the counterion.^{3,18,45} Recent examples of *trans*-III *tetra*-*N*-substituted cyclam complexes with coordinated pendant arms include a bis-methylene-phosphonato nickel(II) complex reported by Blahut *et al.* (CCDC 1430239†),⁴⁶ and the tetraacetamide-cobalt(II) complex described by Bond *et al.* (CCDC 1949780†).⁴⁷

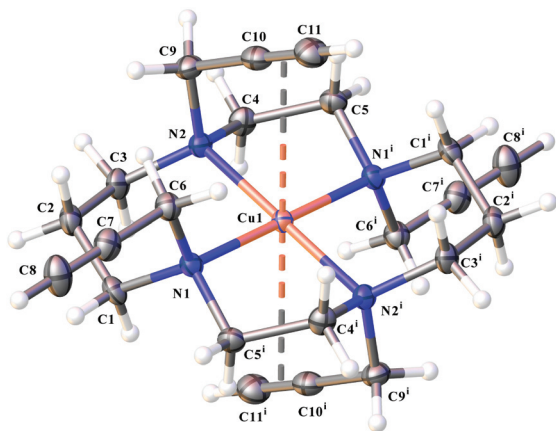


Fig. 8 Olex2 depiction of complex dication **9B** *trans*-III-[Cu(9)]²⁺ with displacement ellipsoids shown at the 50% probability level. The two perchlorate counterions are not shown. The complex dication resides on an inversion site and the superscript 'i' denotes $-x, 1 - y, -z$.

Crystal **9C** was found to contain two distinct [Cu(9)](ClO₄)₂ complex molecules – for convenience labelled as **9C-1** and **9C-2** – and a water molecule. The **9C-1** complex molecule is pseudo-octahedral in character, with weak axial perchlorate coordination *trans* to weak π coordination from an *N*-propargyl residue (Fig. 9 and ESI Fig. SX7a†). The cyclam fragment has a *trans*-I disposition. The metal ion is displaced 0.066(1) Å from the least squares plane defined by the equatorial nitrogen atoms, $-0.184(1)$ Å from the line defined by one of the pairs of opposing nitrogen atoms (N1, N3), and 0.291(1) Å from that of the second pair (N2, N4).

The metal to perchlorate oxygen atom distance is 2.890(2) Å and the metal to π -bond distance is approximately 3.04 Å. The metal to cyclam nitrogen distances range from 2.059(2) to 2.069(2) Å, with the shortest associated with the weakly coordinated alkyne substituent.

The **9C-2** complex molecule is also pseudo-octahedral in character, but with bis axial 1,8-*N*-propargyl π coordination and *trans*-III macrocycle configuration (Fig. 9 and ESI Fig. SX7b†). Residing on an inversion centre, the complex has symmetrical and necessarily weak axial coordination bonds of approximately 2.93 Å. Located on an inversion centre, the unique metal to cyclam nitrogen distances are 2.028(2) and 2.125(2) Å (Table 2).

Both located on inversion sites, the structural features of the pseudo octahedral *trans*-III **9C-2** dication are similar to those of the pseudo octahedral *trans*-III **9B** complex dication (Table 2). Not surprisingly, the structural features of the pseudo octahedral *trans*-I **9C-1** complex cation differ significantly from those of the square pyramidal *trans*-I **9A** perchlorato complex cation.

An unexpected enol ether

The fourth and fifth isolated crystal types, **9D** and **9E** (Fig. 10, ESI Fig. SX8, SX9, and Table SX2†), were found to contain copper cyclam complex cations in which one of the pendant

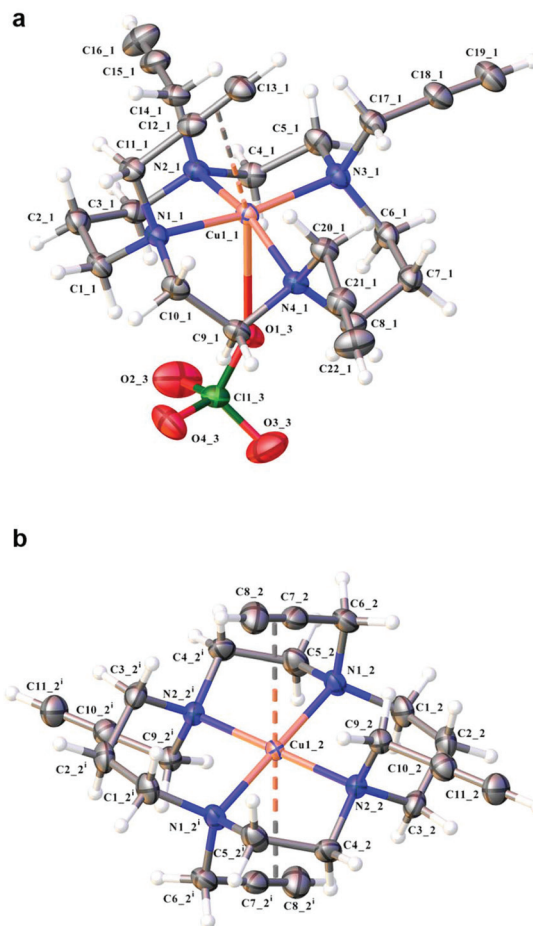


Fig. 9 Olex2 depictions of (a) complex **9C-1** *trans*-I-[Cu(9)](ClO₄)⁺ and (b) complex dication **9C-2** *trans*-III-[Cu(9)]²⁺, with displacement ellipsoids shown at the 50% probability level. The perchlorate counterions are not shown.

propargyl residues is unexpectedly replaced by an enol ether. It would appear that hydroalkoxylation of the alkyne has occurred to form an enol ether, **13**, *via* reaction with the methanol solvent. Recrystallisation of Cu(9) from other alcohols was investigated, but no corresponding hydroalkoxylation reaction was observed in solvents other than methanol.

High resolution mass spectrometry of material from the same crystal batch supports the single crystal structure determinations, returning molecular ion peaks at 223.60899, 224.11072, 224.60813, and 225.10993 ([M]²⁺ for C₂₃H₃₆CuN₄O²⁺ calculated as 223.60925, 224.11039, 224.60780, 225.10948) with the correct isotope patterns.

Differing in colour intensity, the asymmetric unit of **9D** contains a water molecule, while that of **9E** instead contains a methanol solvent molecule. While both have axial ether coordination and a *trans* axial interaction with one of the two perchlorate counterions, there is a significant difference in the nature of their respective perchlorate interactions. The axially positioned perchlorate of **9D** is ordered, while that of **9E** is disordered. Further, the metal to perchlorate oxygen separation in

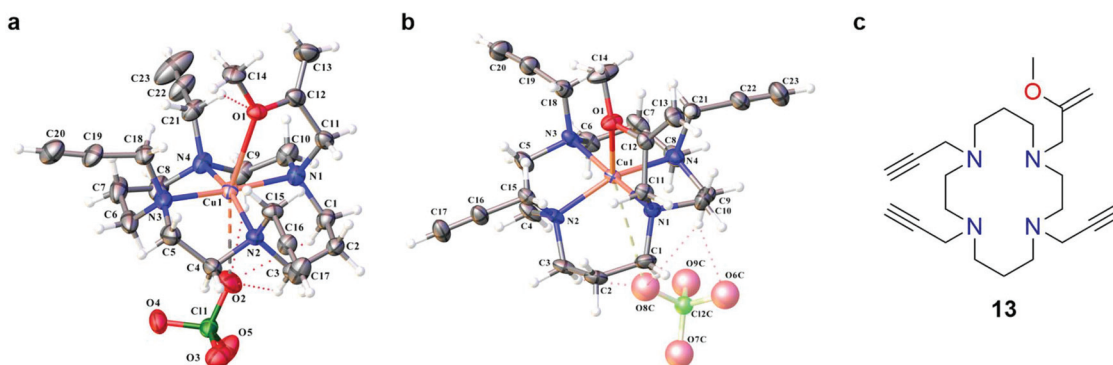


Fig. 10 Olex2 depictions of the structures obtained from (a) crystal **9D** and (b) crystal **9E** of *trans*-1-[Cu(1-(2-methoxyallyl)-4,8,11-tri(prop-2-yn-1-yl)-1,4,8,11-tetraazacyclotetradecane)]²⁺, ([Cu(**13**)]²⁺). Displacement ellipsoids are shown at the 30% and 50% probability level respectively in (a) and (b). The second perchlorate is not shown in both cases, and nor is a water molecule in crystal **9D** and a methanol solvate in crystal **9E**. Disorder is highlighted with 'faded' colours. The formed enol ether **13** is depicted in (c).

Table 3 Selected bond lengths (Å) and angles (°) within the metal coordination sphere observed in structures of the complex [Cu(**13**)](ClO₄)₂, **9D** and **9E**

	9D <i>trans</i> -I	9E ^a <i>trans</i> -I
Cu–N1	2.078(3)	2.084(2)
Cu–N2	2.048(3)	2.047(2)
Cu–N3	2.089(3)	2.109(2)
Cu–N4	2.089(3)	2.057(2)
Cu–O (ether)	2.574(2)	2.607(2)
Cu–O (ClO ₄ [−])	3.200(4)	3.883(10) ^a
N1–Cu–N2	95.16(13)	94.59(9)
N1–Cu–N3	175.37(13)	175.42(9)
N1–Cu–N4	85.52(13)	86.14(10)
N2–Cu–N3	86.09(14)	85.51(9)
N2–Cu–N4	161.59(12)	157.80(9)
N3–Cu–N4	94.70(15)	95.51(10)
N1–Cu1–O (ether)	74.34(11)	74.39(8)
N2–Cu1–O (ether)	99.14(10)	101.87(9)
N3–Cu1–O (ether)	101.07(11)	101.10(8)
N4–Cu1–O (ether)	98.75(11)	99.69(8)
N1–Cu1–O (ClO ₄ [−])	85.92(12)	80.8(2) ^a
N2–Cu1–O (ClO ₄ [−])	83.82(12)	79.41(18) ^a
N3–Cu1–O (ClO ₄ [−])	98.65(12)	103.7(2) ^a
N4–Cu1–O (ClO ₄ [−])	77.88(12)	78.81(18) ^a

^a Disordered perchlorate orientation with shortest metal to oxygen distance.

9D is 3.200(4) Å, whereas the shortest metal to perchlorate oxygen distance in **9E** is 3.883(10) Å (Table 3). While the latter presumably reflects an electrostatic interaction, the shorter distance in **9D** suggests some degree of covalent coordination. The copper to ether oxygen distance in **9D** is 2.574(2) Å, slightly shorter than in **9E** at 2.607(2) Å. The two complex cations are distorted square pyramidal in character, though **9D** may be regarded as pseudo octahedral. The trigonal index (τ) of **9D** is 0.23, while that of **9E** is 0.29. The metal of **9D** is displaced 0.163(1) Å from the least squares plane defined by the equatorial nitrogen atoms, −0.084(1) Å from the line defined by one of the pairs of opposing nitrogen atoms (N1, N3), and 0.331(1) Å from the second pair (N2, N4). The metal of **9E** is

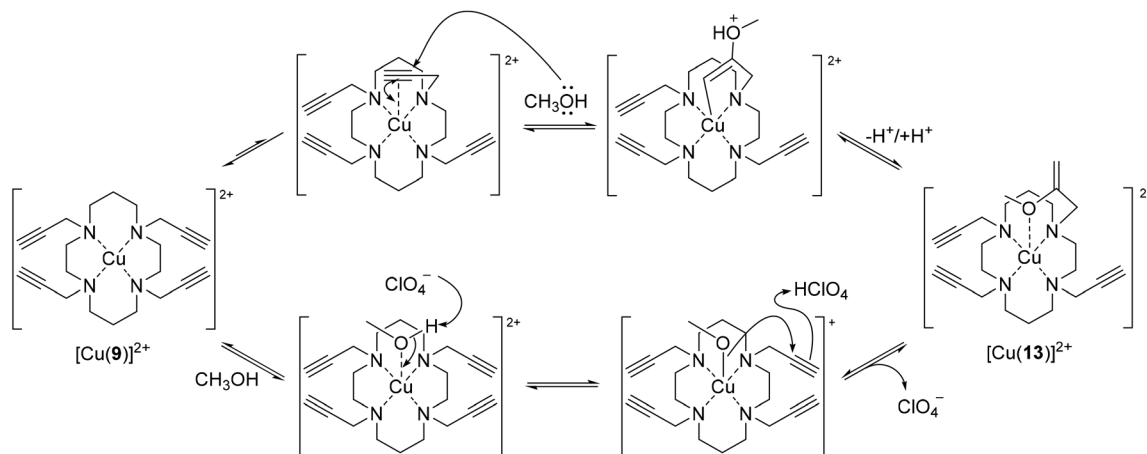
displaced 0.156(1) Å from the least squares plane defined by the equatorial nitrogen atoms, −0.084(1) Å from the line defined by one of the pairs of opposing nitrogen atoms (N1, N3), and 0.395(1) Å from the second pair (N2, N4).

The cyclam nitrogen to copper to ether oxygen angles vary in **9D** from 74.34(11) to 101.07(11)°, and in **9E** they range from 74.39(8) to 101.87(9)°. The metal to cyclam nitrogen distances in **9D** vary from 2.048(3) to 2.089(3) Å, and in **9E** these distances span from 2.047(2) to 2.109(2) Å.

A mechanism for hydroalkoxylation

The intramolecular copper-mediated hydroalkoxylation event observed and characterised by X-ray crystallography is an intriguing outcome. Although various examples of metal-catalysed alkyne hydroalkoxylation reactions have been reported, relatively few of these are intermolecular.⁴⁸ The addition of alcohols to alkynes is typically achieved using a palladium catalyst,⁴⁹ however examples of copper-activated hydroalkoxylation have been reported. Copper-catalysed intramolecular hydroalkoxylation have been used in the synthesis of benzofurans other heteroaromatic systems.^{50,51} Bertz *et al.* reported a rare example of intermolecular hydroalkoxylation, in which ethanol was added to ethyl propiolate in the presence of copper(II) sulfate to generate ethyl 3,3-diethoxypropionate.⁵² While Kang and co-workers recently reported the related reaction of exogenous primary amines (benzyl amine or *n*-propylamine) with pendant alkyne arms on macrocyclic copper(II) and nickel (II) complexes, thus achieving hydroamination of the alkyne pendant.⁵³ There are also parallels between the formation of [Cu(**13**)]²⁺ from [Cu(**9**)]²⁺ and the solvolysis of C≡N bonds in pendant *N*-alkylnitriles by macrocyclic copper(II) complexes reported by Barefield (hydrolysis of nitrile to amide),⁵⁴ and Schröder (methanolysis of nitrile to imino-ether) and co-workers.⁵⁵

We postulate that the metal is required for the observed methanolysis of [Cu(**9**)]²⁺ to [Cu(**13**)]²⁺, as observed by Schröder and co-workers with their nitrile complexes,⁵⁵ and that solvolysis occurs after complexation. We have previously



Scheme 3 Proposed mechanism for formation of enol ether complex $[\text{Cu}(\mathbf{13})]^{2+}$ from the reaction of $[\text{Cu}(\mathbf{9})]^{2+}$ with the solvent methanol. Top: reaction *via* transient alkyne coordination to the metal, which enables attack by methanol on the π system; bottom: reaction to form a copper-alkoxide species *via* coordination of methanol to the metal, followed by nucleophilic attack of this on the uncoordinated alkyne (which approximates to an allowed 5-*exo-dig* cyclisation).

reported a structure for ligand **9** from a crystal obtained by evaporation of a methanolic solution of **9** in the presence of KClO_4 , without any evidence of the methanolysis reaction. In contrast, pure bulk $\text{Cu}(\mathbf{9})$ undergoes this methanolysis reaction when crystallised *via* slow evaporation from methanol solution.

Late transition metal-catalysed alkyne hydroalkoxylation reactions are usually envisaged to proceed *via* coordination of the pendant π system to the metal, which activates the alkyne and enables nucleophilic attack by the alkoxy group.^{56,57} A plausible mechanism for the formation of $[\text{Cu}(\mathbf{13})]^{2+}$ from $[\text{Cu}(\mathbf{9})]^{2+}$ in this way is outlined in Scheme 3. However the structural data obtained for $[\text{Cu}(\mathbf{9})]^{2+}$ reveal only weak coordination between alkyne and the copper centre with ligand **9** in the solid state (crystal **9B**, Fig. 8), with the perchlorate counterion competing for copper coordination with the alkyne (crystal **9A**, Fig. 7). This suggests either that transient alkyne coordination to copper occurs to enable the attack by methanol (Scheme 3, top path), or that the observed hydroalkoxylation follows an alternative mechanism, perhaps *via* formation of a copper-alkoxide species through coordination of methanol to the copper, and nucleophilic attack of this on the uncoordinated alkyne, with perchlorate facilitating the required proton transfer (Scheme 3, bottom path).

UV-visible spectroscopy

UV-visible spectra of $\text{Cu}(\text{II})$ perchlorate complexes of **6–9** in methanol were obtained; absorption maxima are presented in Table 4. The electronic spectrum of each complex exhibits an intense ligand-to-metal charge transfer (LCMT) band in the UV region (264–307 nm),⁵⁸ alongside a comparatively weaker absorption band in the visible region (536–606 nm) corresponding to $\text{Cu}(\text{II})$ d–d transitions. λ_{max} values for all transitions are typical of *N*-alkylated cyclam derivatives.³⁷ A bathochromic shift is observed as the number of functionalised amine

Table 4 Electronic absorption data for $\text{Cu}(\text{II})$ complexes of compounds **6–9** and **14** in CH_3OH (unless otherwise indicated)

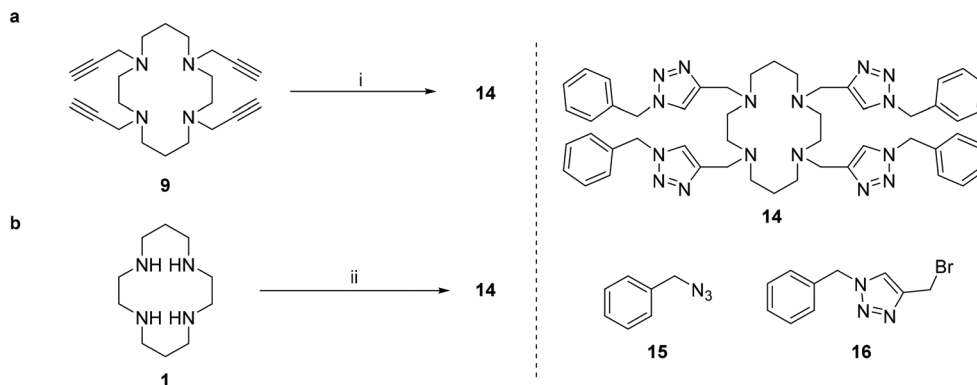
Complex	$\lambda_{\text{max}}/\text{nm}$ ($\epsilon/\text{M}^{-1} \text{cm}^{-1}$)
$[\text{Cu}(\mathbf{6})]^{2+}$	264 (6600), 536 (110)
$[\text{Cu}(\mathbf{7})]^{2+}$	303 (8240), 541 (180)
$[\text{Cu}(\mathbf{8})]^{2+}$	296 (7000), 606 (200)
$[\text{Cu}(\mathbf{9})]^{2+}$	307 (7700), 543 (220)
$[\text{Cu}(\mathbf{14})]^{2+}$	316 (6500), 654 (290) ^a

^a DMF used as solvent.

increases from the mono-*N*-functionalised $[\text{Cu}(\mathbf{6})]^{2+}$, to the complexes of the tetra-*N*-alkylated ligands **7–9**. Little difference in the d–d transition energy is observed between $[\text{Cu}(\mathbf{7})]^{2+}$ and $[\text{Cu}(\mathbf{9})]^{2+}$, which suggests that any $\text{Cu}(\text{II})$ -propargyl interaction which may occur is limited to two pendants. As expected, replacement of a propargyl group with a methyl ester in $[\text{Cu}(\mathbf{8})]^{2+}$ results in a further red shift. The relative strength of the coordination environments around the central $\text{Cu}(\text{II})$ ion exhibited in the structural data (above) is consistent with the d–d transition energies observed in the spectra, with the latter increasing alongside the strength of pendant coordination.

Derivatisation of tetra-propargyl derivative **9**

To demonstrate the utility of **9** as a precursor to more complex tetra-functionalised cyclam derivatives, the ‘tetra-click’ tetra-triazolyl cyclam species **14** was synthesised *via* a copper(I)-catalysed azide–alkyne cycloaddition (CuAAC) of **9** with benzyl azide (Scheme 4a). To minimise the sequestration of the copper(I) catalyst by the macrocyclic starting material and product, copper(I) iodide – relatively insoluble in most organic solvents – was used as a heterogeneous catalyst. Monitoring the reaction mixture *via* mass spectrometry indicated that sequestration of the catalyst did occur to some extent. However, the tetra-click product **14** could be isolated in moder-



Scheme 4 Synthesis of 'tetra-click' tetra-triazolyl cyclam **14**. Reagents and conditions: (i) benzyl azide **15**, CuI, sodium ascorbate, DIPEA, THF, rt, 5 d, 30%; (ii) bromide **16**, H₂O/CH₃CN (1 : 1), NaOH, rt, 16 h, 71%. See synthesis and characterisation section of the ESI† for further details.

ate yield (46% on 100 mg scale, 30% on 0.50 g scale) by collecting the precipitate formed during the reaction and subjecting this directly to flash column chromatography over silica. Accordingly, a convergent route to **14** was developed (Scheme 4b), with a view that an increased yield could be achieved if the CuAAC was conducted in the absence of the cyclam. Bromide **16** was formed in two steps from benzyl azide,⁵⁹ and in the critical step, used to alkylate cyclam **1** in good yield (71%).

The spectroscopic properties of **14** were investigated alongside **9** for comparison. The stoichiometry of complexation of both **9** and **14** with Cu(II) was investigated by UV-visible spectrophotometric titrations, and returned results that are consistent with previous studies on similar cyclam ligands.^{21,28,37} The UV-visible titration of **9** in methanol with Cu(ClO₄)₂ showed the absorbances at 307 and 543 nm steadily increasing with the addition of Cu(ClO₄)₂, to reach their maxima upon the addition of one equivalent of Cu(II) (Fig. 11). No significant increase in absorbance at either wavelengths was observed with further addition of Cu(II). Similar observations were made in the titration of **14** in DMF with Cu(ClO₄)₂ (Fig. 12). Job's

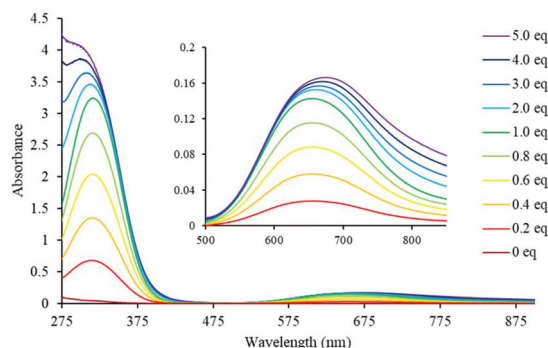


Fig. 12 UV-visible spectrophotometric titrations of **14** (0.5 mM) with Cu(ClO₄)₂ (50 mM) at intervals of 5 min in DMF at 25 °C, with inset enlarging the region between 500–850 nm.

plot experiments confirmed each stoichiometric ratio to be 1 : 1 (Fig. S1, ESI†).

Conclusions

Four *N*-propargyl cyclam ligands have been synthesised and their copper complexes investigated. To the best of our knowledge, crystal **B** of [Cu(**9**)](ClO₄)₂ constitutes the first cyclam derivative to exhibit intramolecular non-acetylide alkyne coordination, although this coordination is weak. Several ligand systems have been reported previously to exhibit monomeric η²-alkyne coordination,^{60,61} including the notable alkyne 'cages',^{62,63} and organometallic acetylide cyclam complexes.^{64,65} Xu and Chao prepared the Nd(III) complex of tetra-*N*-propargyl cyclam, however none of the pendant alkynes were coordinated to the metal in that complex.⁶⁶ Similarly, a variety of alkyne-containing cyclam-based lanthanoid complexes investigated by Milne *et al.* did not exhibit alkyne coordination to the metal.⁶⁷ Ellis *et al.* successfully prepared a series of alkyne-containing *N*-alkylated derivatives of the 9-membered *N,N',N''*-1,4,7-triazacyclononane (TACN) ring system but did not isolate any metal complexes,⁶⁸ whereas

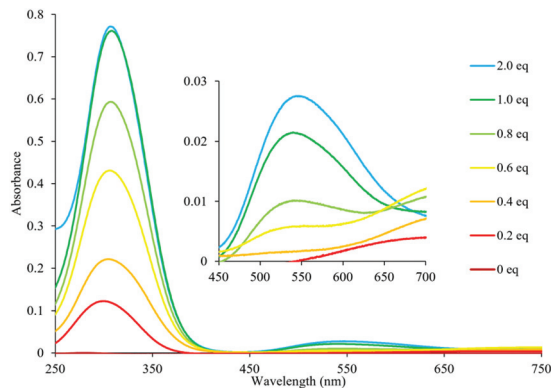


Fig. 11 UV-visible spectrophotometric titrations of **9** (0.1 mM) with Cu(ClO₄)₂ (30 mM) at intervals of 5 min in CH₃OH at 25 °C, with inset enlarging the region between 450–700 nm.

Baker *et al.* have reported a copper(i) complex of the smaller TACN azamacrocycle with an intramolecularly-coordinated pendant alkyne.⁶⁹ A search of the Cambridge Structural Database yields few examples of amine-bound metal ions with a coordinating alkyne connected through the chelator backbone. Aurora *et al.* isolated a Cu(II) polyamido complex containing a *C*-propargyl group which exhibited a weak apical interaction between alkyne and metal with C–Cu distances of 2.805(4) and 2.737(4) Å.⁴² Seebald *et al.* recently reported the structure of a mono-*N*-propargyl cobalt(II) cyclam complex, designed for use as an NMR probe,³¹ and there are a small number of other examples in the literature of more heavily functionalised azamacrocycles bearing pendant *N*-propargyl groups.^{53,70} Intramolecular η^2 -alkyne interactions were also recently observed in a series of coordinated lithium acetylide complexes.⁷¹

In addition, we have isolated multiple crystals of [Cu(9)](ClO₄)₂ from a single crystallisation, with each structure exhibiting a unique coordination complex, configuration, or conformation of the ligand **9**. The formation of a collection of distinct species from a single set of components suggests that the complexes are similar energetically.

Finally the ‘tetra-click’ reaction of **9** with benzyl azide to form tetra-triazole **14** provides proof of concept for the straightforward derivatisation of the tetra-*N*-propargyl ligand **9**, which will enable further developments in the design and synthesis of macrocyclic metal ion sensors, and target-activated metal complexes for biomedical applications.

Experimental

Synthetic procedures

Synthetic procedures and characterisation data for ligands are detailed in the ESI.†

Safety note: Perchlorate salts of metal complexes with organic ligands are potentially explosive. Only small amounts of material should be prepared and these should be handled with caution.

General procedure for preparation of metal complexes. To a solution of *N*-functionalised cyclam (1.0 eq.) in EtOH (0.1 M) was added dropwise a solution Cu(ClO₄)₂·6H₂O (0.8–1.0 eq.) in EtOH (0.1 M) at room temperature. The reaction mixture was heated at reflux for 1 h, cooled on an ice bath and the solvent was decanted. The remaining residue was washed with ice-cold EtOH (3 × 20 mL) and Et₂O (3 × 20 mL), and dried *in vacuo* to give the desired metal complex.

[Cu(6)](ClO₄)₂. Ligand **6** (128 mg, 0.537 mmol) and Cu(ClO₄)₂·6H₂O (160 mg, 0.432 mmol) were complexed according to the general complexation procedure (substituting MeOH for EtOH) to give [Cu(6)](ClO₄)₂ as a purple-pink powder (173 mg, 80%). **M.p.** 264–265 °C. **UV-Vis** (CH₃OH) λ_{max} /nm (ϵ /M⁻¹ cm⁻¹) 264 (6600); 536 (110). **IR** ν_{max} /cm⁻¹ 3548, 3241, 2929, 2888, 1632, 1429, 1367, 1297, 1236, 1057, 619. **HRMS** (ESI+) *m/z* 400.09330, 401.09699, 402.09102, 403.09476, 404.08847, 405.09208 ([M – ClO₄]⁺); calcd for

C₁₃H₂₆ClCuN₄O₄⁺ 400.09331, 401.09667, 402.09150, 403.09486, 404.08855, 405.09191 ([M – ClO₄]⁺). **Anal.** calcd for C₁₃H₂₆Cl₂CuN₄O₈·CH₃OH: C 31.56, N 10.51, H 5.68; found C 31.74, N 10.77, H 5.48. Crystals suitable for single crystal X-ray diffraction were readily grown by slow evaporation of a methanolic solution of the complex.

[Cu(7)](ClO₄)₂. Ligand **7** (20 mg, 0.072 mmol) and Cu(ClO₄)₂·6H₂O (27 mg, 0.072 mmol) were complexed according to the general complexation procedure to give [Cu(7)](ClO₄)₂ as a purple solid (33 mg, 81%). **M.p.** 131–134 °C (decomposed). **UV-Vis** (CH₃OH) λ_{max} /nm (ϵ /M⁻¹ cm⁻¹) 303 (8240); 541 (180). **IR** ν_{max} /cm⁻¹ 3504, 3243, 2936, 2269, 1653, 1477, 1370, 1340, 1072, 996, 956, 931, 861, 835, 797, 727, 673, 620, 537, 497, 469. **HRMS** (ESI+) *m/z* 466.14011, 467.14343, 468.13853, 469.14182, 470.13540, 471.13843 [M – ClO₄]⁺; calcd for C₁₈H₃₂ClCuN₄O₄⁺ 466.14026, 467.14362, 468.13832, 469.14178, 470.13550, 471.13886 [M – ClO₄]⁺. **Anal.** calcd For C₁₈H₃₂Cl₂CuN₄O₈·H₂O: C 36.96, N 9.58, H 5.86; found C 37.12, N 9.51, H 5.51. Crystals suitable for single crystal X-ray diffraction were readily grown by slow evaporation of a solution of the complex in acetonitrile.

[Cu(8)](ClO₄)₂. Ligand **8** (20 mg, 0.052 mmol) and Cu(ClO₄)₂·6H₂O (19 mg, 0.052 mmol) were complexed according to the general complexation procedure to give [Cu(8)](ClO₄)₂ as a blue solid (26 mg, 77%). **M.p.** 118–121 °C (decomposed). **UV-Vis** (CH₃OH) λ_{max} /nm (ϵ /M⁻¹ cm⁻¹) 296 (7000); 606 (200). **IR** ν_{max} /cm⁻¹ 3265, 2971, 2119, 1683, 1603, 1456, 1388, 1340, 1302, 1272, 1252, 1081, 991, 959, 930, 912, 808, 729, 672, 622. **HRMS** (ESI+) *m/z* 548.14545, 549.14882, 550.14322, 551.14656, 552.14069, 553.14391 [M – ClO₄]⁺; calcd for C₂₂H₃₄ClCuN₄O₆⁺ 548.14574, 549.14910, 550.14381, 551.14726, 552.14099, 553.14434 [M – ClO₄]⁺. **Anal.** calcd for C₂₂H₃₄Cl₂CuN₄O₁₀·H₂O: C 39.62, N 8.40, H 5.44. Found: C 39.99, N 8.28, H 5.24. Crystals suitable for single crystal X-ray diffraction were readily grown by slow evaporation of a methanolic solution of the complex.

[Cu(9)](ClO₄)₂. Ligand **9** (50 mg, 0.14 mmol) and Cu(ClO₄)₂·6H₂O (52 mg, 0.14 mmol) were complexed according to the general complexation procedure to give [Cu(9)](ClO₄)₂ as a blue solid (69 mg, 80%). **M.p.** 118–120 °C (decomposed). **UV-Vis** (CH₃OH) λ_{max} /nm (ϵ /M⁻¹ cm⁻¹) 307 (7700); 543 (220). **IR** ν_{max} /cm⁻¹ 3249, 2846, 1678. **HRMS** (ESI+) *m/z* 514.14048, 515.14370, 516.13816, 517.14129, 518.13563, 519.13916 [M – ClO₄]⁺; calcd for C₂₂H₃₂ClCuN₄O₄⁺ 514.14026, 515.14361, 516.13845, 517.14181, 517.14181, 518.13550, 519.13886 [M – ClO₄]⁺. **Anal.** calcd for C₂₂H₃₂Cl₂CuN₄O₈: C 42.97, N 9.11, H 5.25. Found: C 43.23, N 9.12, H 5.21. Spectrometric and elemental analyses were conducted on bulk material isolated from complexation in ethanol according to General Procedure for Preparation of Metal Complexes. The series of unique crystals characterised by X-ray diffraction was obtained *via* slow liquid–liquid diffusion (0.1 M aqueous solution of Cu(ClO₄)₂; 0.1 M methanolic solution of **9**) at room temperature overnight. The described coloured crystal series was attained and identified by eye on all repeated attempts of the diffusion. Suitable single crystal specimens were selected from the crys-

tallisation suspension and attached with Exxon Paratone N oil to a short length of fibre supported on a thin piece of copper wire inserted in a copper mounting pin.

Crystallography

Single crystal X-ray diffraction data were collected on an Agilent SuperNova equipped with an Atlas CCD. The crystal was harvested from amongst the diffusion supernatant, and affixed to a thin mohair fibre attached to a goniometer head with Exxon Paratone N. The crystal was quenched in a continuous stream of dry N₂ regulated by an Oxford Cryosystems Cryostream at 150(2) K. Mirror monochromated Cu-K α radiation from a micro-source was used for data collection. Data reduction and finalisation were conducted with CrysAlisPro.⁷¹ In general, structures were obtained using ShelXS and, in all cases, extended and refined with ShelXL-2018/3.⁷² Computations and image generation were undertaken with the assistance of the WinGX,⁷³ ShelXle⁷⁴ and Olex2⁷⁵ user interfaces. In general, all non-hydrogen atoms were modelled with anisotropic displacement parameters, and a riding atom model applied for hydrogen atoms.

CCDC reference numbers 2012628–2012634 and 2019803.†

Conflicts of interest

There are no conflicts of interest to declare.

Acknowledgements

We acknowledge and pay respect to the Gadigal people of the Eora Nation, the traditional owners of the land on which we research, teach and collaborate at the University of Sydney. M. Yu was supported by a University of Sydney International Scholarship (USydis), and J. Batten by a Research Training Program (RTP) Scholarship from the Australian Government. We acknowledge the facilities and the scientific and technical assistance of Sydney Analytical, a core research facility at The University of Sydney, the Australian Research Council for funding through Discovery Project grant DP120104035, and Professor Cameron Kepert for crystallographic insights.

References

- 1 A. Rodríguez-Rodríguez, Z. Halime, L. M. P. Lima, M. Beyler, D. Deniaud, N. Le Poul, R. Delgado, C. Platas-Iglesias, V. Patinec and R. Tripier, *Inorg. Chem.*, 2016, **55**, 619–632.
- 2 L. Fabbrizzi, in *Macrocyclic and Supramolecular Chemistry: How Izatt-Christensen Award Winners Shaped the Field*, ed. R. M. Izatt, 2016, ch. 8, pp. 165–199.
- 3 K. E. Barefield, *Coord. Chem. Rev.*, 2010, **254**, 1607–1627.
- 4 T. A. Kaden, *Top. Curr. Chem.*, 1984, **121**, 157–179.
- 5 T. L. Mako, J. M. Racicot and M. Levine, *Chem. Rev.*, 2019, **119**, 322–477.
- 6 S. Chowdhury, B. Rooj, A. Dutta and U. Mandal, *J. Fluoresc.*, 2018, **28**, 999–1021.
- 7 P. Comba, L. R. Gahan, G. R. Hanson, V. Mereacre, C. J. Noble, A. K. Powell, I. Prisecaru, G. Schenk and M. Zajackowski-Fischer, *Chem. – Eur. J.*, 2012, **18**, 1700–1710.
- 8 T. J. Hubin, J. M. McCormick, S. R. Collinson, M. Buchalova, C. M. Perkins, N. W. Alcock, P. K. Kahol, A. Raghunathan and D. H. Busch, *J. Am. Chem. Soc.*, 2000, **122**, 2512–2522.
- 9 Y. H. Lau, J. K. Clegg, J. R. Price, R. B. Macquart, M. H. Todd and P. J. Rutledge, *Chem. – Eur. J.*, 2018, **24**, 1573–1585.
- 10 L. Fabbrizzi, F. Foti, M. Licchelli, P. M. Maccarini, D. Sacchi and M. Zema, *Chem. – Eur. J.*, 2002, **8**, 4965–4972.
- 11 J. Martín-Caballero, A. San José Wéry, S. Reinoso, B. Artetxe, L. San Felices, B. El Bakkali, G. Trautwein, J. Alcañiz-Monge, J. L. Vilas and J. M. Gutiérrez-Zorrilla, *Inorg. Chem.*, 2016, **55**, 4970–4979.
- 12 G. Jens, W. Thomas and K. Burkhard, *Curr. Org. Synth.*, 2007, **4**, 390–412.
- 13 J. Zhu, P. M. Usov, W. Xu, P. J. Celis-Salazar, S. Lin, M. C. Kessinger, C. Landaverde-Alvarado, M. Cai, A. M. May, C. Slebodnick, D. Zhu, S. D. Senanayake and A. J. Morris, *J. Am. Chem. Soc.*, 2018, **140**, 993–1003.
- 14 G. Neri, I. M. Aldous, J. J. Walsh, L. J. Hardwick and A. J. Cowan, *Chem. Sci.*, 2016, **7**, 1521–1526.
- 15 T. Hoppe, S. Schaub, J. Becker, C. Würtele and S. Schindler, *Angew. Chem., Int. Ed.*, 2013, **52**, 870–873.
- 16 M. M. Konai, I. Pakrudheen, S. Barman, N. Sharma, K. Tabbasum, P. Garg and J. Haldar, *Chem. Commun.*, 2020, **56**, 2147–2150.
- 17 T. J. Clough, L. Jiang, K. L. Wong and N. J. Long, *Nat. Commun.*, 2019, **10**, 1420.
- 18 J. S. Derrick, J. Lee, S. J. C. Lee, Y. Kim, E. Nam, H. Tak, J. Kang, M. Lee, S. H. Kim, K. Park, J. Cho and M. H. Lim, *J. Am. Chem. Soc.*, 2017, **139**, 2234–2244.
- 19 M. Yu, T. M. Ryan, S. Ellis, A. I. Bush, J. A. Triccas, P. J. Rutledge and M. H. Todd, *Metallomics*, 2014, **6**, 1931–1940.
- 20 P. S. Pallavicini, A. Perotti, A. Poggi, B. Seghi and L. Fabbrizzi, *J. Am. Chem. Soc.*, 1987, **109**, 5139–5144.
- 21 Y. H. Lau, J. R. Price, M. H. Todd and P. J. Rutledge, *Chem. – Eur. J.*, 2011, **17**, 2850–2858.
- 22 S. Ast, P. J. Rutledge and M. H. Todd, *Eur. J. Inorg. Chem.*, 2012, **2012**, 5611–5615.
- 23 J. K.-H. Wong, S. Ast, M. Yu, R. Flehr, A. J. Counsell, P. Turner, P. Crisologo, M. H. Todd and P. J. Rutledge, *ChemistryOpen*, 2016, **5**, 375–385.
- 24 M. Yu, G. Nagalingam, S. Ellis, E. Martinez, V. Sintchenko, M. Spain, P. J. Rutledge, M. H. Todd and J. A. Triccas, *J. Med. Chem.*, 2016, **59**, 5917–5921.
- 25 M. Spain, J. K. H. Wong, G. Nagalingam, J. M. Batten, E. Hortle, S. H. Oehlers, X. F. Jiang, H. E. Murage,

- J. T. Orford, P. Crisologo, J. A. Triccas, P. J. Rutledge and M. H. Todd, *J. Med. Chem.*, 2018, **61**, 3595–3608.
- 26 A. Zhanaidarova, C. E. Moore, M. Gembicky and C. P. Kubiak, *Chem. Commun.*, 2018, **54**, 4116–4119.
- 27 M. Yu, S. Ast, Q. Yu, A. T. S. Lo, R. Flehr, M. H. Todd and P. J. Rutledge, *PLoS One*, 2014, **9**, e100761.
- 28 M. Yu, N. H. Lim, S. Ellis, H. Nagase, J. A. Triccas, P. J. Rutledge and M. H. Todd, *ChemistryOpen*, 2013, **2**, 99–105.
- 29 M. Yu, Q. Yu, P. J. Rutledge and M. H. Todd, *ChemBioChem*, 2013, **14**, 224–229.
- 30 H. Struthers, T. L. Mindt and R. Schibli, *Dalton Trans.*, 2010, **39**, 675–696.
- 31 L. M. Seebald, C. M. DeMott, S. Ranganathan, P. N. Asare-Okai, A. Glazunova, A. Chen, A. Shekhtman and M. Royzen, *J. Inorg. Biochem.*, 2017, **170**, 202–208.
- 32 E. Tamanini, A. Katewa, L. M. Sedger, M. H. Todd and M. Watkinson, *Inorg. Chem.*, 2009, **48**, 319–324.
- 33 E. Tamanini, K. Flavin, M. Motevalli, S. Piperno, L. A. Gheber, M. H. Todd and M. Watkinson, *Inorg. Chem.*, 2010, **49**, 3789–3800.
- 34 F. Boschetti, F. Denat, E. Espinosa, A. Tabard, Y. Dory and R. Guillard, *J. Org. Chem.*, 2005, **70**, 7042–7053.
- 35 I. M. Helps, D. Parker, J. Chapman and G. Ferguson, *J. Chem. Soc., Chem. Commun.*, 1988, 1094–1095.
- 36 A. J. Counsell, A. T. Jones, M. H. Todd and P. J. Rutledge, *Beilstein J. Org. Chem.*, 2016, **12**, 2457–2461.
- 37 M. Yu, J. R. Price, P. Jensen, C. J. Lovitt, T. Shelper, S. Duffy, L. C. Windus, V. M. Avery, P. J. Rutledge and M. H. Todd, *Inorg. Chem.*, 2011, **50**, 12823–12835.
- 38 L. Y. Martin, L. J. DeHayes, L. J. Zompa and D. H. Busch, *J. Am. Chem. Soc.*, 1974, **96**, 4046–4048.
- 39 B. Bosnich, C. K. Poon and M. L. Tobe, *Inorg. Chem.*, 1965, **4**, 1102–1108.
- 40 W. A. Hoffert and M. P. Shores, *Acta Crystallogr., Sect. E: Struct. Rep. Online*, 2011, **67**, m853–m854.
- 41 C. Sun, C. R. Turlington, W. W. Thomas, J. H. Wade, W. M. Stout, D. L. Grisenti, W. P. Forrest, D. G. VanDerveer and P. S. Wagenknecht, *Inorg. Chem.*, 2011, **50**, 9354–9364.
- 42 A. Aurora, M. Boiocchi, G. Dacarro, F. Foti, C. Mangano, P. Pallavicini, S. Patroni, A. Taglietti and R. Zanoni, *Chem. – Eur. J.*, 2006, **12**, 5535–5546.
- 43 A. W. Addison, T. N. Rao, J. Reedijk, J. van Rijn and G. C. Verschoor, *J. Chem. Soc., Dalton Trans.*, 1984, 1349–1356.
- 44 M. Bakaj and M. Zimmer, *J. Mol. Struct.*, 1999, **508**, 59–72.
- 45 P. Moore, J. Sachinidis and G. R. Willey, *J. Chem. Soc., Chem. Commun.*, 1983, 522–523.
- 46 J. Blahut, P. Hermann, A. Gálisová, V. Herynek, I. Císařová, Z. Tošner and J. Kotek, *Dalton Trans.*, 2016, **45**, 474–478.
- 47 C. J. Bond, R. Cineus, A. Y. Nazarenko, J. A. Sperryak and J. R. Morrow, *Dalton Trans.*, 2020, **49**, 279–284.
- 48 A. Corma, V. R. Ruiz, A. Leyva-Pérez and M. J. Sabater, *Adv. Synth. Catal.*, 2010, **352**, 1701–1710.
- 49 F. Alonso, I. P. Beletskaya and M. Yus, *Chem. Rev.*, 2004, **104**, 3079–3160.
- 50 C. Castro, E. Gaughan and D. Owsley, *J. Org. Chem.*, 1966, **31**, 4071–4078.
- 51 N. G. Kundu, G. Chaudhuri and A. Upadhyay, *J. Org. Chem.*, 2001, **66**, 20–29.
- 52 S. H. Bertz, G. Dabbagh and P. Cotte, *J. Org. Chem.*, 1982, **47**, 2216–2217.
- 53 J. Y. Lee, S.-G. Kang and C.-H. Kwak, *Inorg. Chim. Acta*, 2015, **430**, 61–65.
- 54 E. K. Barefield, K. A. Foster, G. M. Freeman and K. D. Hodges, *Inorg. Chem.*, 1986, **25**, 4663–4668.
- 55 L. Tei, A. J. Blake, V. Lippolis, C. Wilson and M. Schröder, *Dalton Trans.*, 2003, 304–310.
- 56 M. Trinchillo, P. Belanzoni, L. Belpassi, L. Biasiolo, V. Busico, A. D'Amora, L. D'Amore, A. Del Zotto, F. Tarantelli, A. Tuzi and D. Zuccaccia, *Organometallics*, 2016, **35**, 641–654.
- 57 M. J. Pouy, S. A. Delp, J. Uddin, V. M. Ramdeen, N. A. Cochrane, G. C. Fortman, T. B. Gunnoe, T. R. Cundari, M. Sabat and W. H. Myers, *ACS Catal.*, 2012, **2**, 2182–2193.
- 58 A. Sornosa Ten, N. Humbert, B. Verdejo, J. M. Llinares, M. Elhabiri, J. Jezierska, C. Soriano, H. Kozłowski, A.-M. Albrecht-Gary and E. García-España, *Inorg. Chem.*, 2009, **48**, 8985–8997.
- 59 D. N. Barsoum, C. J. Brassard, J. H. A. Deeb, N. Okashah, K. Sreenath, J. T. Simmons and L. Zhu, *Synthesis*, 2013, **45**, 2372–2386.
- 60 N. J. Greco, M. Hysell, J. R. Goldenberg, A. L. Rheingold and Y. Tor, *Dalton Trans.*, 2006, 2288–2290.
- 61 H. Lang, K. Köhler and S. Blau, *Coord. Chem. Rev.*, 1995, **143**, 113–168.
- 62 M. V. Baker, D. H. Brown, B. W. Skelton and A. H. White, *Aust. J. Chem.*, 2002, **55**, 655–660.
- 63 A. Kunze, R. Gleiter and F. Rominger, *Chem. Commun.*, 1999, 171–172, DOI: 10.1039/A808068B.
- 64 T. Ren, *Chem. Commun.*, 2016, **52**, 3271–3279.
- 65 J. Nishijo and M. Enomoto, *Inorg. Chem.*, 2013, **52**, 13263–13268.
- 66 H.-B. Xu and H.-Y. Chao, *Inorg. Chem. Commun.*, 2007, **10**, 1129–1131.
- 67 M. Milne, K. Chicas, A. Li, R. Bartha and R. H. E. Hudson, *Org. Biomol. Chem.*, 2012, **10**, 287–292.
- 68 D. Ellis, L. J. Farrugia and R. D. Peacock, *Polyhedron*, 1999, **18**, 1229–1234.
- 69 M. V. Baker, D. H. Brown, N. Somers and A. H. White, *Organometallics*, 2001, **20**, 2161–2166.
- 70 C. Caumes, C. Fernandes, O. Roy, T. Hjelmgaard, E. Wenger, C. Didierjean, C. Taillefumier and S. Faure, *Org. Lett.*, 2013, **15**, 3626–3629.
- 71 H. Osseili, K.-N. Truong, T. P. Spaniol, L. Maron, U. Englert and J. Okuda, *Angew. Chem., Int. Ed.*, 2019, **58**, 1833–1837.
- 72 G. Sheldrick, *Acta Crystallogr., Sect. C: Struct. Chem.*, 2015, **71**, 3–8.
- 73 L. Farrugia, *J. Appl. Crystallogr.*, 2012, **45**, 849–854.
- 74 C. B. Hubschle, G. M. Sheldrick and B. Dittrich, *J. Appl. Crystallogr.*, 2011, **44**, 1281–1284.
- 75 O. V. Dolomanov, L. J. Bourhis, R. J. Gildea, J. A. K. Howard and H. Puschmann, *J. Appl. Crystallogr.*, 2009, **42**, 339–341.